Electronic transport through carbon nanotubes with ferromagnetic electrodes or in magnetic fields

S. KROMPIEWSKI[*]

Institute of Molecular Physics, Polish Academy of Sciences,
M. Smoluchowskiego 17, 60-179 Poznań, Poland

Spin-dependent electronic transport through carbon nanotubes (CNTs) was studied, either sandwiched between ferromagnetic contacts or in external magnetic fields. Attention was paid to the conductance dependence on geometrical size (the length and diameter) of the CNTs, chirality, and conditions at CNT/contact interface. The CNTs are end-contacted to *fcc* (111) metallic leads, and the relative atomic positions at the interfaces are determined by the relaxation procedure. Additionally, a charge neutrality condition is imposed on the extended molecule (i.e., CNT with a few atomic layers of the leads) in order to fix the band line-up of the whole system. Using a single-band tight-binding model and a Green's function technique, it is shown that if the electrodes are ferromagnetic, quite a considerable giant magnetoresistance effect can occur. For paramagnetic electrodes in a parallel magnetic field, clear Aharonov–Bohm oscillations are observed, with distinct minima in the conductance. The depth of the dips depends on the diameters of the CNTs, most likely due to some unintentional doping from the contacts. In the case of perpendicular geometry, pronounced conductance oscillations appear whenever the magnetic length becomes smaller than the perimeter of a CNT.

Key words: *carbon nanotube; electronic transport; magnetoresistance*

1. Introduction

Carbon nanotubes (CNTs) are tubular structures made of graphene (two-dimensional graphite) by rolling it up along the so-called wrapping vector [1]. The wrapping (or chiral) vector, $\mathbf{C}_h$, is fully defined in terms of its components (n, m) in the basis vectors $\mathbf{a}_1 = (0.5a\sqrt{3}, 0.5a)$ and $\mathbf{a}_2 = (0.5a\sqrt{3}, -0.5a)$, where $a = 2.46$ Å is the lattice constant of graphene. Typically, the length of CNTs ranges from several hundred nanometers up to a few micrometers, whereas their cross-sections are quite small and amount only to several nanometers for single-wall (SW) CNTs, and roughly 10 times more for multi-wall (MW) CNTs. Remarkably, the physical properties of the CNTs depend critically on their chirality, that is, on the manner in which they fold up

_____

[*]E-mail: stefan.krompiewski@ifmpan.poznan.pl

from the pristine graphene plane. CNTs whose chiral vector components fulfil the condition that n–m is divisible by 3 are metallic, otherwise they are semiconducting. Metallicity (or lack thereof) is fully related to the electronic structure of nanotubes and the absence (presence) of energy gaps. To see how the so-called zone folding proceeds, let us start with a graphene energy spectrum:

$$E(\vec{k}) = \pm t \sqrt{1 + 4\cos\frac{3k_x a}{2}\cos\frac{k_y a}{2} + 4\cos^2\frac{k_y a}{2}} \tag{1}$$

where t is the nearest neighbour transfer (hopping) integral, regarded hereafter as the energy unit. Now, in order to obtain the band structure of a CNT, one simply imposes cyclic boundary conditions on the chiral vector $\mathbf{C}_h$, and the $\mathbf{k}$ vector becomes quantised according to $\mathbf{C}_h \mathbf{k} = 2\pi j$, $j = 1, 2, \dots$. Specifically, in the case of the armchair SWCNT, $\mathbf{C}_h = (n, n)$, one finds:

$$E(k_y, j) = \pm t \sqrt{1 + 4\cos\frac{k_y a}{2}\cos\frac{j\pi}{n} + 4\cos^2\frac{k_y a}{2}} \tag{2}$$

Similarly, for another most fundamental symmetry, the zigzag with $\mathbf{C}_h = (n, 0)$, the results reads:

$$E(k_x, j) = \pm t \sqrt{1 + 4\cos\frac{3k_x a}{2}\cos\frac{j\pi}{2} + 4\cos^2\frac{j\pi}{2}} \tag{3}$$

It can be easily seen that, in agreement with what has been stated before, armchair CNTs are always metallic, in contrast to zigzag ones, which have a gap unless n is a multiple[*] of 3. Undoped CNTs have a Fermi energy at $E = 0$ (charge neutrality point), and the valence (lower) bands cross the conductance (upper) bands in metallic CNTs exclusively at $k = \pm 2\pi/3a$ and 0 for the wrapping vectors (n, n) and $(3i, 0)$, respectively. This observation suggests that metallic CNTs can be easily driven to a semiconducting state upon applying external disturbances such as mechanical strain or magnetic field. Both theoretical and experimental studies fully confirm this suggestion [2–5]. In this paper, attention is directed to the physical properties of CNTs, which might be utilized in emerging spin electronics – spintronics. Attention is therefore directed to the effect of magnetic field on electronic transport through CNTs, as well as to so-called giant magnetoresistance (GR) observed when CNTs are sandwiched between ferromagnetic electrodes. The paper is organized in the following way. In Sec. 2 the mathematical apparatus and simulation method of the devices of interest are described, followed by results elucidating size and chirality effects. Sec. 3 is devoted to the GMR effect and Sec. 4 shows results on the conductance of CNTs in

---

[*]Incidentally, even for zigzag CNTs with modulo $(n, 3) = 0$ it is straightforward to show that in the case of anisotropic hopping integrals, $t_\perp \neq t_\parallel$, a narrow gap does open.

the presence of either parallel or perpendicular magnetic fields. Finally, Sec. 5 summarizes the main results of the paper.

2. The method and geometrical aspects

The method is based on a single-band tight-binding model and is applied to both $p_z(\pi)$ electrons in CNTs and s electrons in metal-electrodes. In general, computations are performed within the non-equilibrium Green's function method (see e.g. [6] and references therein), using the following relations for the Green's function (g), electron density matrix (ρ), and current (I), with L, R, and C referring to the left and right electrodes and the CNT itself, respectively:

$$g = \left(E - H_C - \Sigma_L - \Sigma_R \right)^{-1}$$ (4)

$$\rho = \frac{1}{2\pi} \int dE\, g(f_L \Gamma_L + f_R \Gamma_R) g^\dagger$$ (5)

$$I = \frac{e}{h} \int dE\, (f_L - f_R)\, Tr(\Gamma_L g \Gamma_R g^\dagger)$$ (6)

where $\Gamma_a = i(\Sigma_a - \Sigma_a^\dagger)$, $\Sigma_a = T_{Ca} g_a T_{Ca}^\dagger$, and f_a is the Fermi function with the chemical potential $\mu_a = \mu \pm eV/2$ for $a = L, R$. Additionally, T_{Ca} is the matrix that couples the CNT to the a-th electrode, V stands for the voltage, and g_a is the surface Green's function of the infinite lead, E denotes energy, and H_C – Hamiltonian of an isolated CNT. The electric current I yields a differential conductance $G = dI/dV$, which in the equilibrium case, $V = 0$, reduces to the well-known Landauer–Büttiker formula

$$G = \frac{e^2}{h} Tr(\Gamma_L g \Gamma_R g^\dagger)$$ (7)

The devices of interest here are CNTs end-contacted to metal electrodes. They are simulated as described in [7]. It is noteworthy that the structures in question are relaxed using the Lennard–Jones potential in order to find energetically favourable positions of carbon atoms with respect to electrode atoms. During the relaxation process, the external electrodes are allowed to rotate and shift independently of each other, and in the case of double-wall (DW) CNTs the inner carbon tube is also free to rotate. The nearest neighbour hopping integrals are kept constant (equal to t) within the cut-off radii throughout the whole system, whereas inter-tube hopping is set to

$$t_{\text{int}} = -\frac{t}{8} \cos\theta_{ij} \exp\left(\frac{d_{ij} - b}{\delta} \right)$$ (8)

where θ_{ij} stands for the angle between the π orbitals, d_{ij} is the relative distance, and the two remaining constants are $\delta = 0.45$ Å and $b = 3.34$ Å [8]. In order to line up the

Fermi energies of the CNTs and the model electrodes, the charge neutrality requirement has been imposed on the so-called extended molecule consisting of the CNT and two closest atomic planes from each electrode. The charge has been calculated from Eq. (5) in a self-consistent way by shifting all the on-site potentials of the extended molecule so as to ensure global charge neutrality at $E_F = 0$.
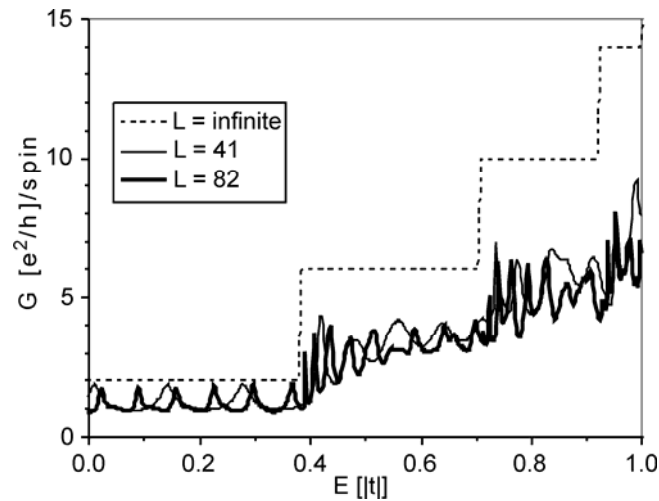

Fig. 1. Conductance of the armchair SWCNT (8,8) as a function of energy. The dashed line corresponds to a pristine (ideal infinite) CNT, whereas the thin (thick) curve to one with finite length, and $L = 41$ carbon rings ($L = 82$ carbon rings). Note a periodic behaviour below $E \approx 0.4$, and a halving of the period as the length doubles
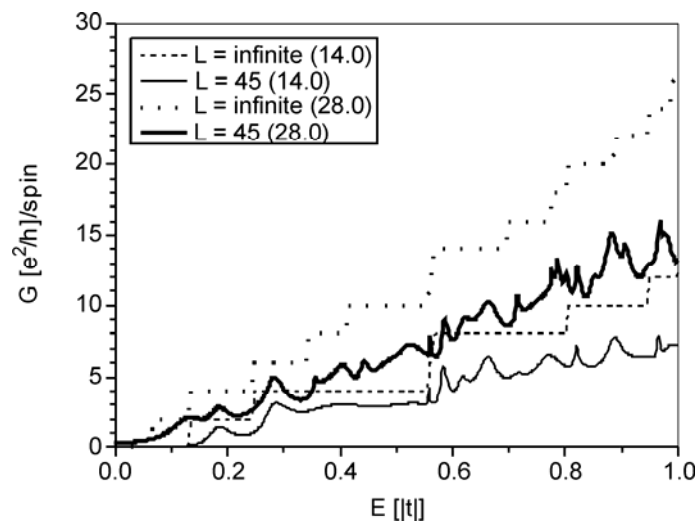

Fig. 2. Conductance spectra for 2 zigzag tubes with different diameters. The stepped curves represent pristine tubes, and the others correspond to $L = 45$ carbon rings. Thick (thin) lines apply to the larger (smaller) diameters

Figures 1 and 2 present the effect of length, diameter, and chirality on the electrical conductance of SWCNTs. As a reference, pristine nanotubes infinite in length are also shown, and they are purely ballistic conductors quantised in integer multiples of the fundamental conductance unit e^2/h (per spin). It is readily seen from Fig. 1 that in the vicinity of the charge neutrality point ($E_F = 0$) the conductance is a periodic function of energy, with a period inversely proportional to the length. Otherwise, the conductance is strongly reduced when compared to that of an infinite CNT. They are also quite irregular, but still reveal some extra features at energies corresponding to van Hove singularities (or steps) of the latter. Figure 2 shows that in the case of semiconducting zigzag nanotubes the "memory" about van Hove singularities seems to be lost rather quickly as the diameter increases. Another observation is that the region of small conductance narrows with increasing diameter due to the onset of new subbands. In fact, these results show that nominally semiconducting CNTs can become slightly metallic due to doping by the electrodes. The doping depends in general on the work functions of the involved materials (carbon vs. the electrode metal) and on the area of the contact region, so it is the most effective for ultra-short CNTs with a high percentage of atoms at the interface.

3. Giant magnetoresistance

If electrodes are ferromagnetic and the spin-diffusion length is long enough, the giant magnetoresistance effect can occur (for an excellent review on spin-transport in nanoscopic systems see Ref. [9]). Here, it is defined as GMR = $(G_{\uparrow\uparrow} - G_{\uparrow\downarrow})/G_{\uparrow\uparrow}$, where the arrows $\uparrow\uparrow$ and $\uparrow\downarrow$ denote aligned and anti-aligned magnetization orientations of the electrodes.

Motivated by recent experimental findings [10–12] which show that the magnetoresistance of ferromagnetically contacted carbon nanotubes reveals a peculiar behaviour, including the appearance of the so-called inverse GMR for some samples, the present author has studied such systems for several years [6, 7, 13, 14]. The studies were carried out in the quasi-ballistic regime, although most of the hitherto existing experiments concern the diffusive regime and highly resistive devices. It turns out, however, that the ferromagnetic electrodes can also form low resistive junctions with CNTs. This was demonstrated in [15], where MWCNTs were sandwiched between electrodes made of the ferromagnetic alloy $Pd_{1-x}Ni_x$ ($x \approx 0.7$), and shown to have resistances below 100 kΩ at room temperature.

Figure 3 presents the conductance and GMR for a double-wall carbon nanotube, which consists of 45 zigzag rings and 39 armchair rings (45–(5, 0)@39–(8, 8)). The corresponding lengths are then roughly the same (ca. 5 nm each), so both the inner and outer tubes can be regarded as being contacted to the magnetic electrodes. Quantum oscillations are inherent in quantum transport phenomena, yet in the case of MWCNT they are often reported to be washed-out by disorder coming from inter-wall interactions [16, 17]. To mimic a possible effect of disorder, conductance curves have

been energy-averaged. The averaged curves, along with the resultant GMR (dashed), are drawn with solid lines. The averaging was made over the energy-level spacing, which is the most obvious energy-scale in this context.
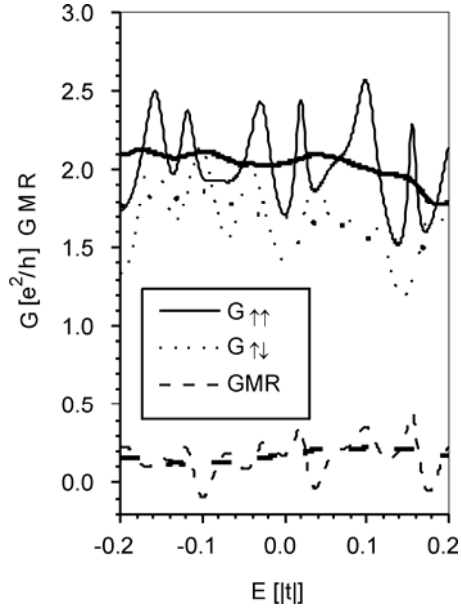

Fig. 3. Conductance and GMR for a double-wall carbon nanotube, which consists of 45 zigzag rings and 39 armchair rings (45-(5,0)@39-(8,8)). The energy averaged conductance (over energy bins equal to the energy-level spacing) and resulting GMR are depicted by thick lines. The averaging mimics the anticipated effect of disorder
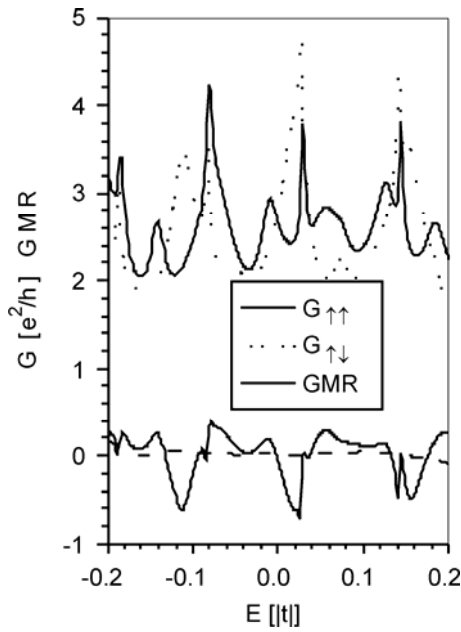

Fig. 4. Conductance and GMR for an armchair DWCNT (3,3)@ (8,8). There are 39 (38) carbon rings in the outer (inner) tube, so that the inner tube is out of contact with the drain. The thick dashed line is defined as in Fig. 3

In order to gain deeper insight into the role of the inner tube, Fig. 4 depicts the results for the pure armchair DWCNT (38–(3, 3)@39–(8, 8)). The inner tube in this

case is by one inter-ring spacing (half the lattice constant) shorter than the outer tube and is out of contact with the drain electrode. Hence, the systems presented in Figs. 3 and 4 are similar, since the zigzag nanotube (5, 0), as a semiconductor, also does not conduct (due to the energy gap in the interval $|E/t| < 0.2$). The most important conclusion to be drawn from this comparison is that the former DWCNT has a much larger and more robust GMR at the neutrality point than the latter one, which happens to change the sign at E_F and reveals large conductance fluctuations. A more detailed analysis [7] shows that these peculiarities originate from inter-tube quantum interference effects and would be suppressed if t_{int} were allowed to vanish.

4. Carbon nanotubes in magnetic fields

Recently, two seminal papers have been published on the magnetoconductance of CNT-based devices [4, 5]. The papers were motivated by theoretical predictions that a magnetic field can drastically modify the electronic band structure [1, 3], including periodic opening (closing) of energy gaps and a splitting of van Hove singularities in the density of states. In this section, an attempt is made to generalize the hitherto existing theoretical studies (restricted to free CNTs) by taking into account the presence of electrodes and accompanying charge transfer processes. Within the tight-binding method, a magnetic field can be most conveniently implemented by the well-known Peierls substitution, $t \rightarrow t\exp[i(2\pi/\Phi_0)\xi]$, where the phase factor is given by [1]:

$$\xi = \frac{\Delta x}{C_h} \Phi \tag{9}$$

$$\xi = \left(\frac{C_h}{2\pi}\right)^2 \frac{B \Delta y}{\Delta x} \left[\cos\frac{2\pi x}{C_h} - \cos\frac{2\pi(x + \Delta x)}{C_h}\right] \tag{10}$$

and for the parallel and axial magnetic field orientations. Above, Φ is a magnetic flux penetrating the cross-section of the CNT, Φ_0 is the magnetic flux quantum, B denotes a uniform static magnetic field, whereas x (Δx) and y (Δy) stand for circumferential and axial coordinates (increments), respectively. Figure 5 presents magnetoconductance spectra computed from Eq. (7) at the global charge neutrality point for 3 armchair nanotubes with different diameters. At a perpendicular field (Fig. 3a), there are conductance oscillations that show an interesting structure with the number of peaks increasing regularly with the diameter. Since on one hand for the increasing diameter the curvature of CNTs decreases, and on the other hand in strong magnetic fields the magnetic length $l = [\Phi_0/(2\pi B)]^{1/2}$ becomes smaller than the perimeter C_h, the CNT electron band structure approaches roughly that of graphene. The observed features can be identified as typical interference patterns (the first sharp peak in Fig. 5a always appears for $l < C_h/2$). For the parallel configuration, Aharonov–Bohm oscillations are clearly visible, with a constant period of Φ_0. The presence of external electrodes manifests
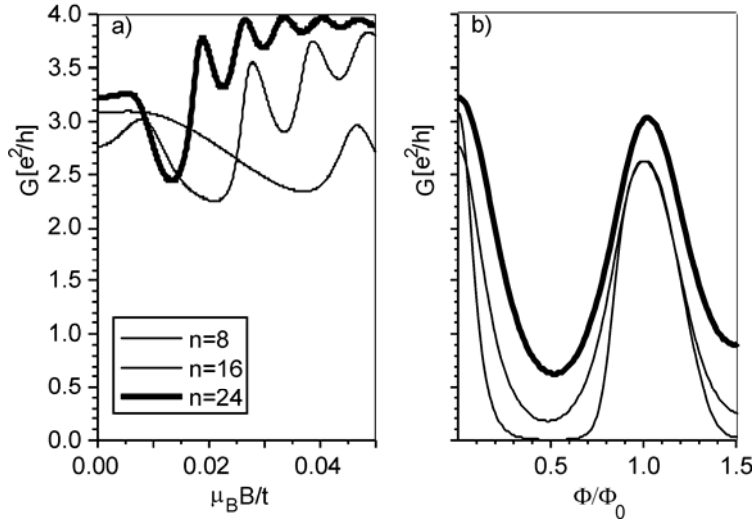
Fig. 5. Magnetoconductance of single-wall CNTs versus dimensionless magnetic
field and flux for perpendicular (a) and parallel (b) orientations. B is normalized
to the hopping parameter, and Φ to the magnetic flux quantum

itself by doping and broadening of the energy levels which make a complete opening
of the gap no longer possible.

5. Conclusions

In this work, the effect of external leads (electrodes) on quantum transport through
carbon nanotubes was analysed. The studies included both geometrical aspects
(length, diameter, and chirality of CNTs) and those essential for spintronic applica-
tions, i.e. the use of ferromagnetic electrodes and the application of magnetic fields.
In general, the GMR effect is quite considerable and may reach several tens of per-
cent. It is, however, very sensitive to the internal structure of the MWCNT and de-
pends on the chirality of the inner tubes and inter-tube interactions. This applies even
to the case when the current flows mainly through the outer tube and the inner tubes
are either decoupled from one of the electrodes or have a gap in the transport energy
window. Regarding the influence of magnetic fields, it was shown that electrode-
induced doping modifies magnetoconductance spectra for parallel fields without
changing the period of Aharonov-Bohm oscillations. The magnetoconductance spec-
tra of CNTs at perpendicular fields, in turn, reveal pronounced oscillations with a
period that scales with the diameter of the CNT.

References

[1] SAITO R., DRESSELHAUS M.S., DRESSELHAUS G., *Physical Properties of Carbon Nanotubes*, Imperial College Press, London, 1998.

[2] MINOT D.E., YAISH Y., SAZONOVA V., PARK J.-Y., DRINK M., MCEUEN P.L., Phys Rev. Lett., 90 (2003), 156401.

[3] AJIKI H., , ANDO T., J. Phys. Soc. Jpn., 62 (1993), 1255.

[4] ZARIC S., OSTOLIC G.N., KONO J., SHAVER J., MOORE V.C., STRANO M.S., HAUGE R.H., SMALLEY R.E., WEI X., Science, 304 (2004), 1129.

[5] COSKUN U.C., WEI T.-C., VISHVESHWARA S., GOLDBART P.M., BEZRYADIN A., Science, 304 (2004), 1132.

[6] KROMPIEWSKI S., J. Magn. Magn. Mater., 272–276 (2004), 1645.

[7] KROMPIEWSKI S., Phys. Stat. Sol. (b), 242 (2005), 226.

[8] ROCHE S., TRIOZON F., RUBIO A., MAYOU D., Phys. Rev. B, 64 (2001), 121401.

[9] SANVITO S., *Handbook of Computational Nanotechnology*, American Scientific Publ. (Stevenson Ranch, CA, 2005); also cond-mat/0503445.

[10] TSUKAGOSHI K., ALPHENAAR B.A., AGO H., Nature (London), 401 (1999), 572.

[11] ZHAO B., MÖNCH I., MÜHL T., SCHNEIDER C.M., Appl. Phys. Lett., 80 (2002), 3144.

[12] JENSEN A., NYGÅRD J., BORGGREEN J., [in:] *Toward the Controllable Quantum* States, Proc. Internat. Symp. Mesoscopic Superconductivity and Spintronics, H. Takayanagi, J. Nitta (Eds.), World Scientific, Singapore, 2003, 33–37.

[13] KROMPIEWSKI S., J. Phys.: Condens. Matter, 16 (2004), 2981.

[14] KROMPIEWSKI S., GUTIERREZ R., CUNIBERTI G., Phys Rev. B, 69 (2004), 155423.

[15] SAHOO S., KONTOS T., SCHÖNENBERGER C., SÜRGERS C., Appl. Phys. Lett., 86 (2005), 112109.

[16] TRIOZON F., ROCHE S., RUBIO A., MAYOU D., Phys. Rev. B, 69 (2004), 121410.

[17] STOJETZ B., MIKO C., FERRÓ L., STRUNK C., Phys Rev. Lett., 94 (2005), 186802.